

UNIVERSIDADE ESTADUAL DE CAMPINAS  
SISTEMA DE BIBLIOTECAS DA UNICAMP  
REPOSITÓRIO DA PRODUÇÃO CIENTÍFICA E INTELECTUAL DA UNICAMP

**Versão do arquivo anexado / Version of attached file:**

Versão do Editor / Published Version

**Mais informações no site da editora / Further information on publisher's website:**

<https://aip.scitation.org/doi/10.1063/1.4866323>

**DOI: 10.1063/1.4866323**

**Direitos autorais / Publisher's copyright statement:**

©2014 by AIP Publishing. All rights reserved.

DIRETORIA DE TRATAMENTO DA INFORMAÇÃO

Cidade Universitária Zeferino Vaz Barão Geraldo

CEP 13083-970 – Campinas SP

Fone: (19) 3521-6493

<http://www.repositorio.unicamp.br>

# Metal gate work function tuning by Al incorporation in TiN

L. P. B. Lima,<sup>1,2,3</sup> H. F. W. Dekkers,<sup>1</sup> J. G. Lisoni,<sup>1</sup> J. A. Diniz,<sup>2</sup> S. Van Elshocht,<sup>1</sup> and S. De Gendt<sup>1,3</sup>

<sup>1</sup>*Imec, Kapeldreef 75, 3000 Leuven, Belgium*

<sup>2</sup>*School of Electrical and Computer Engineering and Center for Semiconductor Components, University of Campinas, P. O. Box 6101, 13083-970 Campinas-SP, Brazil*

<sup>3</sup>*Chemistry Department, KU Leuven, Leuven, Belgium*

(Received 27 November 2013; accepted 7 February 2014; published online 21 February 2014)

Titanium nitride (TiN) films have been used as gate electrode on metal-oxide-semiconductor (MOS) devices. TiN effective work function (EWF) values have been often reported as suitable for pMOS. For nMOS devices, a gate electrode with sufficient low EWF value with a similar robustness as TiN is a challenge. Thus, in this work, aluminum (Al) is incorporated into the TiN layer to reduce the EWF values, which allows the use of this electrode in nMOS devices. Titanium aluminum (TiAl), Al, and aluminum nitride (AlN) layers were introduced between the high-k ( $\text{HfO}_2$ ) dielectric and TiN electrode as Al diffusion sources. Pt/TiN (with Al diffusion) and Pt/TiN/TiAl/TiN structures were obtained and TiN EWF values were reduced of 0.37 eV and 1.09 eV, respectively. The study of TiN/AlN/ $\text{HfO}_2$ /SiO<sub>2</sub>/Si/Al structures demonstrated that AlN layer can be used as an alternative film for TiN EWF tuning. A decrease of 0.26 eV and 0.45 eV on TiN EWF values were extracted from AlN/TiN stack and AlN/TiN laminate stack, respectively. AlN/TiN laminate structures have been shown to be more effective to reduce the TiN work function than just increasing the AlN thickness. © 2014 AIP Publishing LLC.  
[\[http://dx.doi.org/10.1063/1.4866323\]](http://dx.doi.org/10.1063/1.4866323)

## I. INTRODUCTION

Current metal-oxide-semiconductor field effect transistors (MOSFET's) are relying on a high-k gate dielectric. Since the introduction of  $\text{HfO}_2$  as a high-k gate dielectric, Titanium nitride (TiN) has been used as a gate metal electrode due to the thermo dynamical stability with  $\text{HfO}_2$ . Film properties, such as conductivity and work function, are important elements in complementary MOS (CMOS) technology and are therefore widely studied.<sup>1–6</sup> The TiN effective work function (EWF) values have been often reported as suitable for pMOS. For nMOS devices, the challenge is to obtain a gate electrode with sufficient low EWF with a similar robustness as TiN. Physical and electrical properties of TiN films are highly related to film composition. Literature also reports TiN as a mid-gap work function film.<sup>2,3</sup> Variations on TiN properties have been reported for different deposition processes.<sup>7</sup> Several techniques such as chemical vapor deposition (CVD), physical vapor deposition (PVD), and sputtering have been investigated for obtaining TiN films. Nowadays, atomic layer deposition (ALD) system is being widely used for TiN deposition due to the requirement of conformal layers for 3D channel structures, like tri-gates and finFET's. ALD usually provides stoichiometric TiN, resulting in EWF values in the range of 4.7–4.9 eV, adequate for pMOS. Solutions for the nMOS EWF in the range of 4.1–4.4 eV can be obtained by doping the TiN film with different materials (such as Al and N).<sup>8–10</sup> Literature reports had shown that the addition of Al ions into TiN layer can significantly change the TiN EWF.<sup>8,10</sup> The metal gate EWF shift is related to formation of different dipoles at the interface between metal gate and high-k due Al diffusion.<sup>8</sup> The

amount of Al ions at the interface between high-k dielectric and TiN layer will determine the shift on metal gate work function and a decrease of 0.60 eV on TiN EWF can be achieved using Al diffusion approach.<sup>8</sup> In addition, the Al diffusion technique for lowering the metal gate EWF deviates from the “gate last” method due to high temperatures (more than 400 °C) process for Al diffusion.<sup>8,11–13</sup> In this sense, the Al diffusion is often used for a “gate first” approach. Aluminum and TiAl films have been used as an Al diffusion source for tuning the metal gate electrode work function.<sup>8,10</sup> The objective of this work is to decrease the TiN EWF by the incorporation of Al into TiN metal electrode using an AlN layer between  $\text{HfO}_2$  and TiN films as an alternative material for Al diffusion source. The usage of AlN to control the metal gate EWF has been reported as a promising approach for work function engineering for CMOS technology.<sup>11–13</sup> In addition, it is well known that on  $\text{HfO}_2$ /AlN stack is thermally stable at high temperatures.<sup>11</sup> Furthermore, the metal gate EWF is highly dependent on the AlN structure and composition.<sup>13</sup> Low metal gate EWF values can be expected with an increase of Al concentration in AlN layers, and high metal gate EWF can be achieved by increasing the amount of N<sub>2</sub> in the AlN layer.<sup>12,13</sup> Aluminum nitride films are usually obtained by PVD, ALD, and sputtering depositions.<sup>12–15</sup> In this work, the  $\text{HfO}_2$ , AlN, and TiN layers were deposited *in situ* by an ALD system in order to study the influence of Al diffusion at the interface between  $\text{HfO}_2$  and TiN to lower the metal gate EWF. Thermally stability control of Al diffusion into TiN and conformality are advantages of using  $\text{HfO}_2$ /AlN/TiN stack deposited by ALD. In contrast, TiAl is today only reported to be deposited using PVD, which lacks conformal deposition in trenches and fin

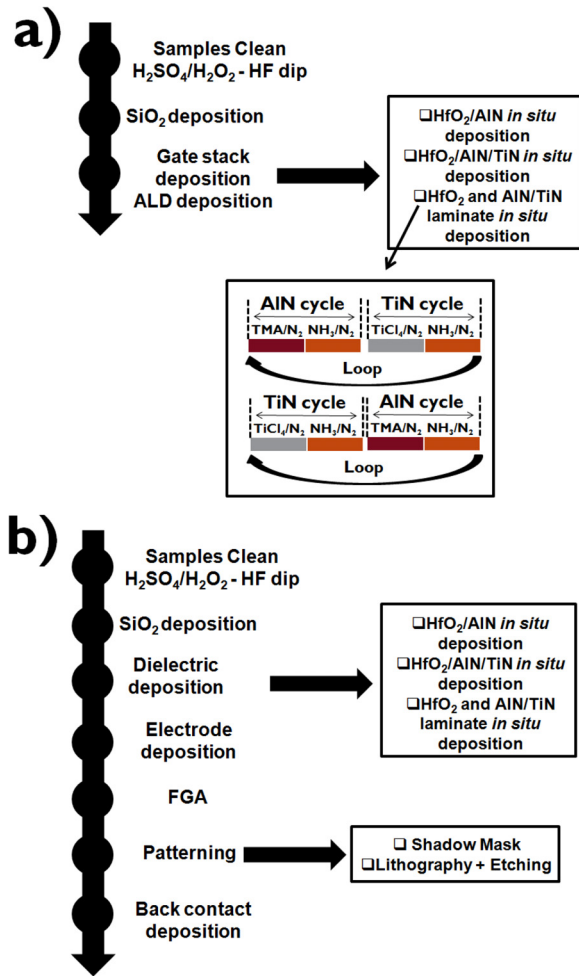


FIG. 1. The fabrication steps for (a) HfO<sub>2</sub>/AlN, HfO<sub>2</sub>/AlN/TiN (with and without laminate) structures; (b) MOS devices.

structures. Therefore, the usage of AlN/TiN stack is more suitable for 3D technology, such as finFET's.

## II. EXPERIMENTAL

The HfO<sub>2</sub>, AlN, and TiN films sequences *in situ* using ALD. ALD of AlN was performed using separate pulses of trimethyl aluminum (TMA) and NH<sub>3</sub> at 400 °C, while for TiN deposition pulses of TiCl<sub>4</sub> and NH<sub>3</sub> were used at 400 °C. The HfO<sub>2</sub> films were deposited on Si (100) p-type wafers. To study the AlN growth, AlN was deposited directly on the top of HfO<sub>2</sub> and also on TiN to examine difference in growth inhibition. The same is done for TiN on the top of AlN. Layers were deposited *in situ* to avoid and minimize

the oxygen contamination. Figure 1(a) presents the fabrication steps for AlN/TiN (first layer is AlN followed by TiN film) and TiN/AlN (first layer is TiN then AlN film) films and laminates. The laminate samples were obtained by switching the precursors (TMA and TiCl<sub>4</sub>) on ALD chamber for several loops, as shown in Figure 1(a). So, the formation of TiAlN film can be achieved using the laminate AlN/TiN and TiN/AlN layers and incorporation of Al into TiN layer, in order to decrease the TiN work function. X-ray reflection (XRR) measurements were used to obtain the film thickness. X-ray photoelectron spectroscopy (XPS) and Secondary ion mass spectrometry (SIMS) were used to investigate the TiN composition and Al incorporation in the TiN layer. The XPS measurements were carried out using Al K $\alpha$  X-ray source (1486.6 eV) with a spot size of 400  $\mu$ m. The film sputtering was performed using Ar<sup>+</sup> ions with energy of 500 eV. The SIMS measurement was used to study the film composition and determine the Al diffusion profile into TiN layer. SIMS measurements were performed using a 500 eV O<sup>2+</sup> ion beam with angle of 44°.

Figure 1(b) shows the process steps for fabrication of MOS capacitors. 2 nm of HfO<sub>2</sub> was deposited on Si (100) wafers covered with SiO<sub>2</sub>. Various SiO<sub>2</sub> thicknesses, between 1.4 and 5.7 nm, were achieved using the slant etch procedure.<sup>14</sup> For calibration of capacitance-voltage (C-V) and EWF extraction routines, reference device (see Table I) was fabricated using Pt sputtering deposition (see Figure 1(b)). Table I shows the sample name, metal gate structure, purpose and metal EWF for capacitors with different metal gate structures. To study the influence of Al incorporation on TiN layer capacitors with metal electrode structures of TiN/TiAl/TiN and TiN/AlN were fabricated. For Pt reference sample (see Table I), 10 nm of TiN and 2 nm of TaN were deposited *in situ* by ALD. The Al layer was deposited on the top of TaN film, followed by a forming gas anneal (FGA) step at 420 °C for 20 min for Al diffusion into TiN film. After the etch of Al film, 70 nm of Pt layer was deposited on top of TaN, as shown in Figure 1(b). For devices with TiN/TiAl/TiN/HfO<sub>2</sub> stack, the TiN and TiAl were deposited by ALD and PVD, respectively. Forming gas anneal was performed after the deposition of this stack. Then, 70 nm of Pt layer was deposited on top of TiN, as shown in Figure 1(b). To obtain TiN/AlN device (see Table I), AlN and TiN depositions were done *in situ* with the HfO<sub>2</sub> deposition. In order to increase the TiN thickness for C-V measurements, 10 nm TiN was deposited on the top of ALD TiN using PVD. After that, a thermal annealing step was performed using forming gas at 420 °C for 20 min, which

TABLE I. Sample name, structure, gate stack deposition, and metal EWF.

Sample name	Structure	Purpose	Gate stack deposition	Metal EWF (eV)
Pt ref	Pt/HfO <sub>2</sub> /SiO <sub>2</sub> /Si	Reference sample for EWF extraction	HfO <sub>2</sub> deposition	5.60
TiN ref	Pt/TiN/HfO <sub>2</sub> /SiO <sub>2</sub> /Si	TiN EWF for reference	HfO <sub>2</sub> /TiN deposition	5.05
Al dif.	Pt/TaN/TiN/HfO <sub>2</sub> /SiO <sub>2</sub> /Si	TiN EWF with Al diffusion	HfO <sub>2</sub> /TiN/TaN deposition	4.68
TiN/TiAl	Pt/TiN/TiAl/TiN/HfO <sub>2</sub> /SiO <sub>2</sub> /Si	TiN EWF using TiAl as a Al diffusion source	HfO <sub>2</sub> /TiN/TiAl/TiN deposition	4.13–3.96
TiN/AlN	TiN/AlN/HfO <sub>2</sub> /SiO <sub>2</sub> /Si	TiN EWF using AlN as a Al diffusion source	HfO <sub>2</sub> /AlN/TiN deposition	5.01–4.78
Laminate	TiN/AlN/HfO <sub>2</sub> /SiO <sub>2</sub> /Si laminate	TiN EWF using AlN laminate as a Al diffusion source	HfO <sub>2</sub> /AlN/TiN laminate deposition	4.85–4.59

corresponds to the standard annealing time for CMOS devices in back end of line (BEOL) process. Separate capacitors, with sizes of  $2500 \mu\text{m}^2$ ,  $10\,000 \mu\text{m}^2$ , and  $78\,400 \mu\text{m}^2$ , were obtained by etching the TiN and AlN after lithographic patterning. Finally, following the  $\text{SiO}_2$  removal from the backside of the silicon wafer, 500 nm Al was deposited by PVD on the backside of the silicon wafer. TiN EWF was extracted using C-V measurements performed on MOS capacitors. C-V measurements were taken from TiN/AlN devices, with and without the laminate deposition, at a frequency of 100 kHz using a Keithley analyzer 4200 SCS model. TiN work function was determined using Hauser's CVC program.<sup>16</sup> The Pt reference device was fabricated as described in Figure 1(b) and was used for calibrate the EWF routine.

### III. RESULTS AND DISCUSSION

Figure 2 shows the growth of AlN layer on  $\text{HfO}_2$  and TiN. The growth per cycle (GPC) was obtained using the XRR thickness. The growth behavior of AlN layer is independent of the surface either when growing onto  $\text{HfO}_2$  or TiN. Indeed, the growth is linear with GPC's of 0.042 nm/cycle. The Al:N ratio as measured by XPS was  $\sim 1$  for the 1.2 nm AlN (Figure 2(b)). The AlN layer formation is confirmed by the presence of Al 2p and N 1s, however, the stoichiometry of AlN is distorted due to native oxidation. The incorporation of Al into TiN has been quantified by SIMS Al implantation experiments ( $2 \times 10^{13}$

atoms/ $\text{cm}^2$  at 5 keV). The Al diffusion profile was obtained by SIMS measurement on a TiN/AlN sample (with structure TiN/AlN/ $\text{HfO}_2$ / $\text{SiO}_2$ /Si) after forming gas anneal, see Figure 2(c). The AlN thickness was about 2 nm. For this TiN/AlN sample, two layers of TiN were used: (i) the first one was deposited *in situ* with  $\text{HfO}_2$  and AlN by ALD; and (ii) the second TiN layer was deposited on the top of the ALD TiN *ex-situ* by PVD. The diffusion of Al ions on TiN layer is shown by the  $^{27}\text{Al}$  presence inside the TiN layer, the presence of  $^{48}\text{Ti}$  evidences that the mixing does not fully consume the TiN films. Moreover, there is no clear difference from the TiN and AlN layer at the interface between those two films which suggests the formation of a TiAlN compound.

To calibrate the EWF extraction routine, the Pt and TiN EWF were extracted from the reference sample. The EWF values obtained were 5.60 eV and 5.05 eV, respectively, in good correspondence with values reported in the literature.<sup>8,17</sup> From Al dif. devices (see Table I) the extracted TiN EWF value was about 4.68 eV. Using TiAl as an Al diffusion source, low TiN work function values around 4.1–4.2 eV can be expected.<sup>10</sup> The extracted TiN EWF from TiN/TiAl devices with 5 nm of TiAl was 3.96 eV, while for the same metal gate stack with 2 nm of TiAl the TiN EWF value was about 4.13 eV. Literature reports that a reduction of 0.60 eV on TiN EWF can be achieved using TiAl layer,<sup>10</sup> but the TiN work function shift is dependent on thickness of TiN film and TiAl. Thus, the extracted TiN work function values from

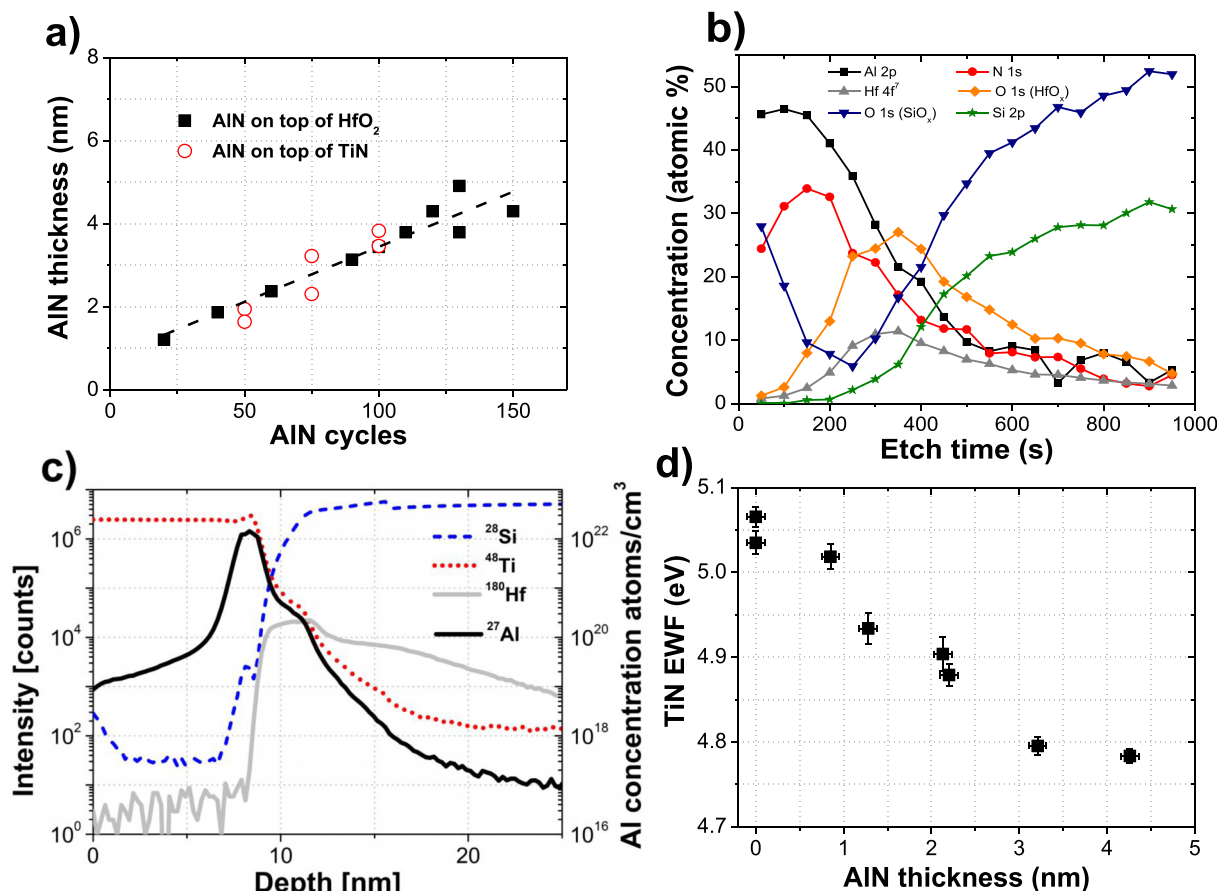


FIG. 2. (a) AlN thickness and AlN mass versus AlN cycles AlN/ $\text{HfO}_2$ / $\text{SiO}_2$ /Si structures; (b) XPS measurement on 1.2 nm of AlN (on top of  $\text{HfO}_2$ ); (c) SIMS measurement on a structure TiN/AlN/ $\text{HfO}_2$ / $\text{SiO}_2$ /Si after forming gas anneal; (d) TiN EWF versus the AlN thickness for laminate structures.



the Al dif. and TiN/TiAl devices show that Al incorporation in TiN layer decreases the metal gate work function. Also the different reduction on TiN EWF, 0.37 eV for Al films and 1.09 eV for TiAl films were observed and are related to different TiN film thickness on those two structures. Figure 2(d) presents the TiN EWF *versus* AlN thickness. We found that the thicker the AlN film on the lower the TiN EWF, clearly pointing out that Al can diffuse from the AlN layer, decreasing the TiN EWF similar to what has been reported for the case of pure Al.<sup>18</sup> The diffusion of Al into TiN layer could generate additional dipole at the interface between the metal gate electrode and high-k gate dielectric, which could lead in lower values for TiN EWF.<sup>8</sup> However, for thicker AlN layers, the Al diffusion into TiN film could be limited and reduced by the high Al concentration on the interface between the AlN and TiN. Thus, the decrease on TiN work function does not change much for thicker AlN layers, as it can be seen for thickness of 3.2 nm (TiN EWF = 4.79 eV) and 4.2 nm (TiN EWF = 4.78 eV). Moreover, the equivalent oxide thickness (EOT) value was not increased which indicates that the Al is diffusing into TiN layer.

Figure 3(a) presents the AlN/TiN laminate structure (with AlN as on top of  $\text{HfO}_2$ ) mass and thickness *versus* AlN cycles graphs. The growth of AlN/TiN laminate per loop also presents a linear growth. Moreover, the slope for the samples with 5 and 10 cycles of TiN presented the same

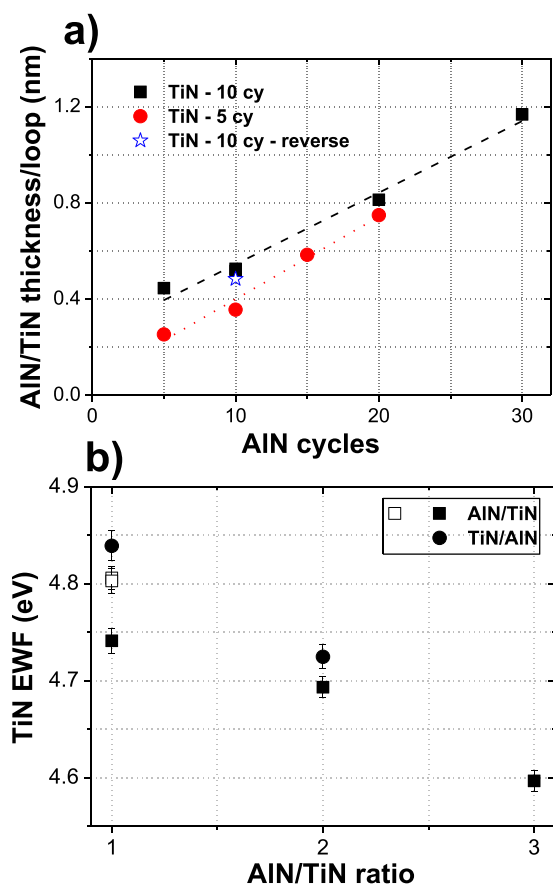


FIG. 3. (a) AlN/TiN thickness *versus* AlN cycles for TiN/AlN/ $\text{HfO}_2$ / $\text{SiO}_2$ /Si laminate. TiN-10cy-reverse means that the first layer of the laminate is TiN instead of AlN; (b) TiN EWF *versus* the AlN/TiN ratio for laminate devices. The open symbols are for laminate structures deposited with 5 loops.

value, which means that the growth of TiN and AlN is the same on both structures. Also, there is no significant difference on AlN/TiN growth if the first layer of the laminate structure is a TiN structures, which confirms the previous conclusion from Figure 2(a). Figure 3(b) presents the TiN EWF *versus* the AlN/TiN ratio for laminate structures. The AlN/TiN laminate ratio consists on the ratio of AlN and TiN cycles on laminate structure, for example, the AlN/TiN ratio of 1 presents the same number of cycles for AlN and TiN depositions, while the AlN/TiN ratio of 3 presents the three times more cycles for AlN than TiN cycles. In addition, increasing the AlN/TiN ratio, the amount of Al is also increased due the higher thickness of AlN layer, but the deposition parameters were set up in order to achieve the same final thickness of laminate structure. For devices with AlN/TiN laminate deposition, the TiN EWF decreases with an increase on number of AlN/TiN ratio, resulting on an increase of AlN thickness per loop. Nevertheless, lower values for TiN work function can be achieved using the laminate deposition. The lowest TiN EWF value of 4.59 eV was extracted from the laminate device with thicker AlN/TiN stack. This indicates that the laminate deposition is more efficient for Al diffusion, the FGA is more effective on thinner layers, than the single AlN layer under TiN film. Furthermore, for the laminate devices with AlN as first deposited layer, the extracted TiN work function presented lower values than for laminate devices with TiN as first layer. Thus, it might be possible that the dipoles at the interface between high-k dielectric and metal electrode present different symmetries for TiN/AlN/ $\text{HfO}_2$  and AlN/TiN/ $\text{HfO}_2$  structures, leading to different effects on the TiN EWF. In summary, the Al diffuses through TiN layer, which result in a decrease on metal electrode work function value.<sup>18</sup> Low values for TiN EWF can be achieved using AlN as an Al diffusion source. A decrease of 0.26 eV and 0.45 eV on TiN work function value were extracted from AlN/TiN stack and AlN/TiN laminate stack, respectively. So, the AlN/TiN laminate structures have been shown to be more effective to reduce the TiN work function than just increasing the AlN thickness. Moreover, all the TiN EWF values are applicable for CMOS technology.<sup>19,20</sup>

#### IV. CONCLUSION

Low values for TiN work function can be achieved using Al diffusion into TiN layer. Literature reports that TiAl and Al layers have been used as an Al diffusion source. A reduction of 1.09 eV on TiN EWF was obtained using TiAl on top of TiN. This was likely to be induced by Al diffusion into TiN (near  $\text{HfO}_2$ ). Indeed, 10 nm TiN yields only to a 0.37 eV TiN EWF decreasing. In addition, the study of TiN/AlN devices demonstrated that AlN layer can be used for TiN EWF tuning. The SIMS measurements confirmed the Al diffusion into TiN film. The diffusion of Al into TiN layer could generate additional dipole at the interface between the metal gate electrode and high-k gate dielectric, which could lead in lower values for TiN EWF. Also, with an increase on AlN thickness a decrease on TiN EWF was observed. Nevertheless, the Al diffusion into TiN film could

be limited and reduced by the high Al concentration on the interface between the AlN and TiN. In addition, a decrease of 0.26 eV and 0.45 eV on TiN work function value were extracted from AlN/TiN stack and AlN/TiN laminate stack, respectively. So, the AlN/TiN laminate structures have been shown to be more effective to reduce the TiN work function than just increasing the AlN thickness. Moreover, all the TiN EWF values are suitable for CMOS technology. Finally, this work shows that Al diffusion into TiN can be used for metal gate work function tuning.

## ACKNOWLEDGMENTS

This work was supported by CNPq (Programa Ciência Sem Fronteiras).

- <sup>1</sup>Y. Liu, T. Hayashida, and T. Matsukawa, *Jpn. J. Appl. Phys., Part 1* **47**, 2433 (2008).
- <sup>2</sup>L. P. B. Lima, J. Diniz, I. Doi, and J. Godoy Filho, *Microelectron. Eng.* **92**, 86 (2012).
- <sup>3</sup>I. Polishchuk, P. Ranade, T. J. King, and C. Hu, *IEEE Electron Device Lett.* **22**, 444 (2001).
- <sup>4</sup>S. H. Hsu, H. C. Chang, C. L. Chu, Y. T. Chen, W. H. Tu, F. J. Hou, C. H. Lo, P. J. Sung, B. Y. Chen, G. W. Huang, G. L. Luo, C. W. Liu, C. Hu, and F. L. Yang, *IEEE Int. Electron Devices Meet.* **2012**, 23.6.1.
- <sup>5</sup>G. S. Kar, L. Breuil, P. Blomme, H. Hody, S. Locorotondo, N. Jossart, O. Richard, H. Bender, G. Van den Bosch, I. Debussechere, and J. Van Houdt, *IEEE Int. Electron Devices Meet.* **2012**, 17.
- <sup>6</sup>T. Matsukawa, Y. Liu, W. Mizubayashi, J. Tsukada, H. Yamauchi, K. Endo, Y. Ishikawa, S. O'uchi, H. Ota, S. Migita, Y. Morita, and M. Mashara, *IEEE Int. Electron Devices Meet.* **2012**, 8.2.1.
- <sup>7</sup>L. P. B. Lima, J. Diniz, C. Radtke, M. V. P. dos Santos, I. Doi, and J. Godoy Filho, *J. Vac. Sci. Technol. B* **31**(5), 052202 (2013).
- <sup>8</sup>X.-R. Wang, Y.-L. Jiang, Q. Xie, C. Detavernier, G.-P. Ru, X.-P. Qu, and B.-Z. Li, *Microelectron. Eng.* **88**, 573 (2011).
- <sup>9</sup>C. L. Hinkle, R. V. Galatage, R. A. Chapman, E. M. Vogel, H. N. Alshareef, C. Freeman, M. Christensen, E. Wimmer, H. Niimi, A. Li-Fatou, J. B. Shaw, and J. J. Chambers, *Appl. Phys. Lett.* **100**, 153501 (2012).
- <sup>10</sup>A. Veloso, S. A. Chew, Y. Higuchi, L. A. Ragnarsson, E. Simoen, T. Schram, T. Witters, A. Van Ammel, H. Dekkers, H. Tielens, K. Devriendt, N. Heylen, F. Sebaai, S. Brus, P. Favia, J. Geypen, H. Bender, A. Phatak, M. S. Chen, X. Lu, S. Ganguli, Y. Lei, W. Tang, X. Fu, S. Gandikota, A. Noori, A. Brand, N. Yoshida, A. Thean, and N. Horiguchi, *Jpn. J. Appl. Phys., Part 1* **52**, 04CA02 (2013).
- <sup>11</sup>M. P. Agustin, H. Alshareef, M. A. Quevedo-Lopez, and S. Stemmer, *Appl. Phys. Lett.* **89**, 041906 (2006).
- <sup>12</sup>H. N. Alshareef, H. F. Luan, K. Choi, H. R. Harris, H. C. Wen, M. A. Quevedo-Lopez, P. Majhi, and B. H. Lee, *Appl. Phys. Lett.* **88**, 112114 (2006).
- <sup>13</sup>M. Hasan, H. Park, J. M. Lee, and K. Hwang, *Electrochem. Solid-State Lett.* **11**(5), h124-h126 (2008).
- <sup>14</sup>Y. J. Lee and S. W. Kang, *J. Vac. Sci. Technol. A* **21**, L13 (2003).
- <sup>15</sup>V. S. Kaushik, B. J. O'Sullivan, G. Pourtois, N. Van Hoornick, A. Delabie, S. Van Elshocht, W. Deweerdt, T. Schram, L. Pantisano, E. Rohr, L. A. Ragnarsson, S. De Gendt, and M. Heyns, *IEEE Trans. Electron Devices* **53**(10), 2627 (2006).
- <sup>16</sup>W. K. Hensen, K. Z. Ahmed, E. M. Vogel, J. R. Hauser, J. J. Wortman, R. D. Venables, M. Xu, and D. Venables, *IEEE Electron Device Lett.* **20**, 179 (1999).
- <sup>17</sup>A. V. Gavrikov, A. A. Knizhnik, A. A. Bagatur'yants, B. V. Potapkin, L. R. C. Fonseca, M. W. Stoker, and J. Schaeffer, *J. Appl. Phys.* **101**, 014310 (2007).
- <sup>18</sup>F. Panciera, S. Baudot, K. Hoummada, M. Gregoire, M. Juhel, and D. Mangelinck, *Appl. Phys. Lett.* **100**, 201909 (2012).
- <sup>19</sup>R. Chau, M. Doczy, B. Doyle, S. Datta, G. Dewey, J. Kavalieros, B. Jin, M. Metz, A. Majumdar, and M. Radosavljević, *Microelectron. Eng.* **80**, 1 (2005).
- <sup>20</sup>R. Chau, M. Doczy, B. Doyle, S. Datta, G. Dewey, J. Kavalieros, B. Jin, M. Metz, A. Majumdar, and M. Radosavljevic, "Advanced CMOS transistors in the nanotechnology era for high-performance, low-power logic applications," *Proceedings of the 7th International Conference on Solid-State and Integrated Circuits Technology (ICSICT), Beijing, China, Oct. 2004*, pp. 26–30.